Electronic Supplementary Material (ESI) for Nanoscale.
This journal is © The Royal Society of Chemistry 2022

SUPPLEMENT DATA

The use of advanced spectral imaging to reveal nanoparticle identity in the biological samples

Qamar A. Alshammari[*,1,2], Rajasekharreddy Pala[*,1], Ayan K. Barui[1], Saud O. Alshammari[1,3], Andromeda M Nauli[4], Nir Katzir[5], Ashraf M. Mohieldin[1], and Surya M. Nauli[1,6]

[*]Authors contribute equally
[1]Department of Biomedical & Pharmaceutical Sciences, Harry and Diane Rinker Health Science Campus, Chapman University, 9401 Jeronimo Road, Irvine, CA 92618-1908, USA
[2]Department of Pharmacology and Toxicology, Faculty of Pharmacy, Northern Border University, KSA.
[3]Department of Plant Chemistry and Natural Products, Faculty of Pharmacy, Northern Border University, KSA
[4]Department of Pharmaceutical Sciences, College of Pharmacy, Marshall B. Ketchum University, Fullerton, CA, USA.
[5]Applied Spectral Imaging, 5315 Avenida Encinas, Suite 150, Carlsbad, CA 92008.
[6]Department of Medicine, University of California Irvine, Irvine, CA 92868, USA.

Corresponding author:
Surya M. Nauli
Chapman University
University of California Irvine
9401 Jeronimo Road.
Irvine, CA 92618-1908
Tel: 714-516-5480
Fax: 714-516-5481
Email: nauli@chapman.edu; snauli@uci.edu

Supplement Figure 1

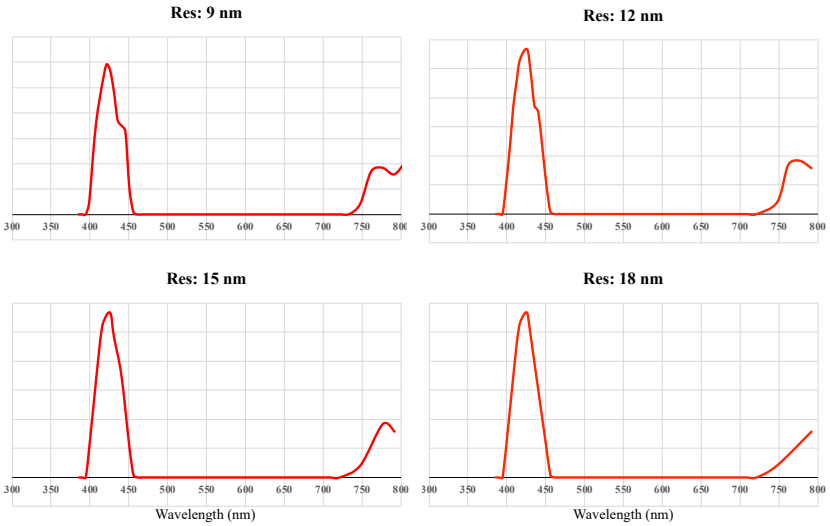

Supp Fig 1. An improved resolution of spectra imaging.
The shell of Ag-NPs was captured using spectral imaging at various resolutions (Res) of 9, 12, 15 and 18 nm. As resolution improves, more detailed changes can be analyzed to further refine the accuracy of the image analysis. A resolution of 9 nm was used throughout our studies.

Supplement Figure 2

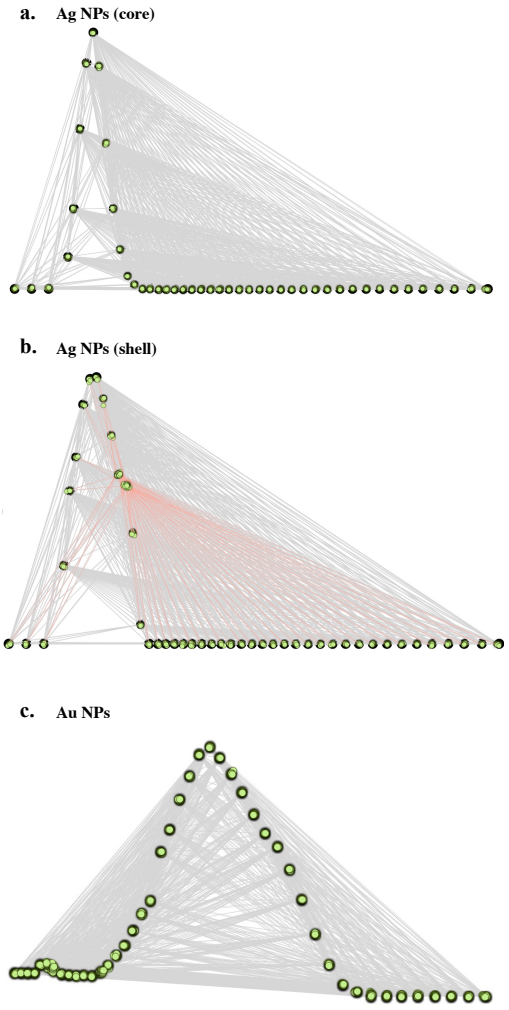

Supp Fig 2. A robust and rigorous analyses of spectra points
The identity (fingerprinting) of a molecule is analyzed based on the relative interactions among 45 spectral points for the core of Ag NPs (**a**), shell of Ag NPs (**b**) and Au NPs (**c**). These 45 points were generated from a spectral resolution of less than 10 nm between 400 nm and 800 nm. The 45 spectral points result in unique 990 interactions as indicated in the gray-color lines. Recognition artificial intelligence is used to improve spectral analysis by studying these unique interactions. As such, our analysis is able to specifically recognize about 90 distinct interactions to differentiate between core and shell of Ag NPs as indicated in the red-color lines.

Supplement Figure 3

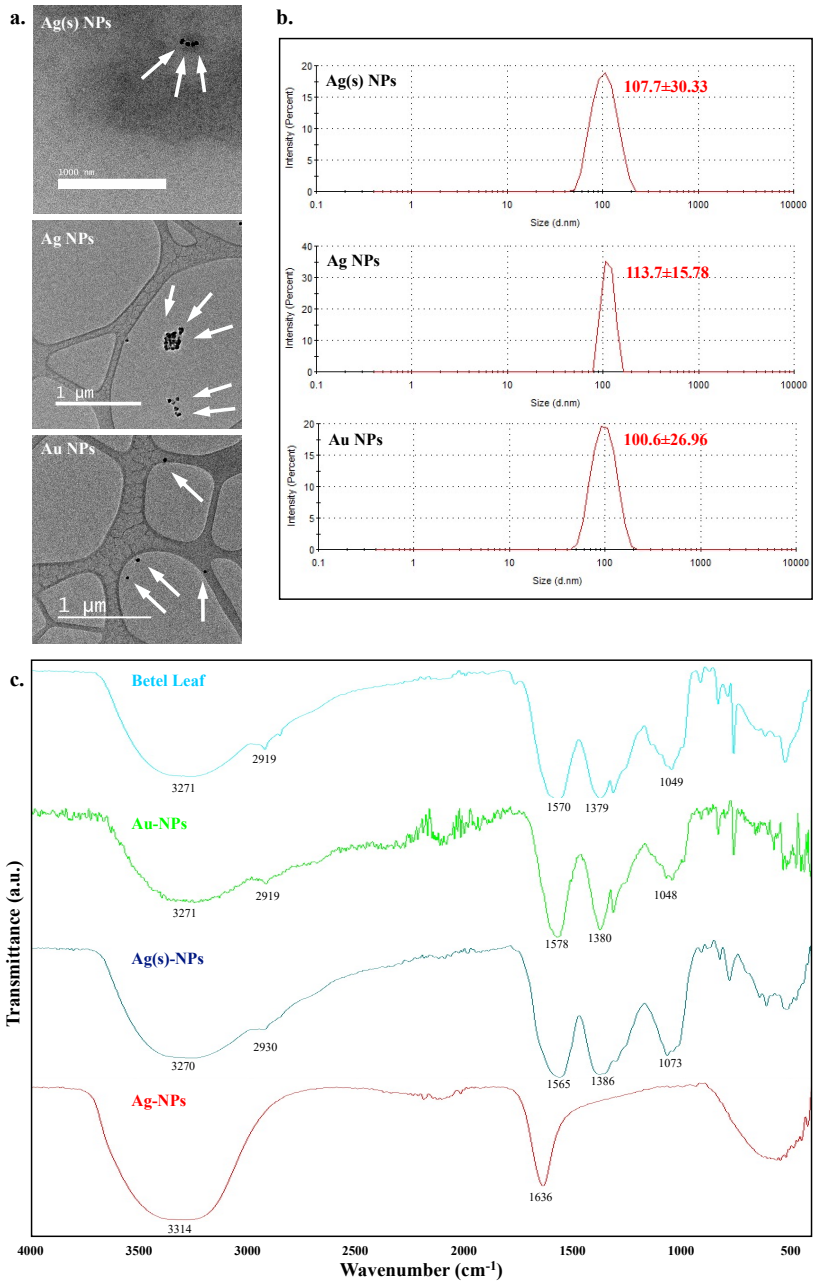

Supp Fig 3. Characterizations of different types of NPs
(a) The white arrows point to nanoparticles (NPs). (**b**) Dynamic light scattering shows the size of NPs (hydrodynamic diameter in nm; d). (**c**). Spectra taken from Fourier-transform infrared spectroscopy reveal key peaks representing polyphenols (O-H stretching; aromatic C-C=C stretching), carboxylic acids (O-H bending), protein molecules (N-H stretching; N-H bending) and H-O-H scissor of water molecules. Please see Method for details.

Supplement Figure 4

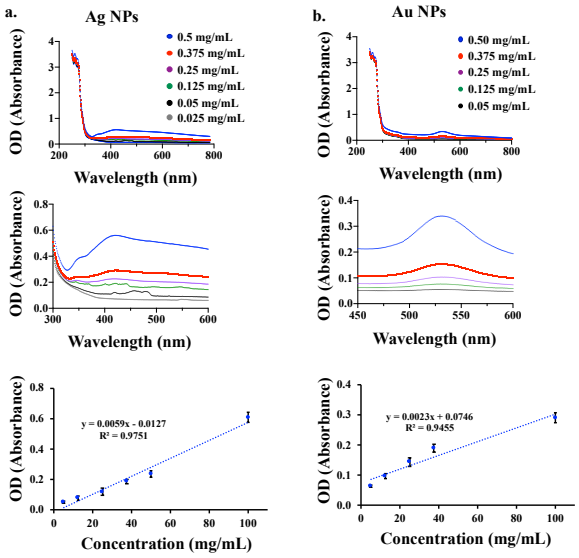

Supp Fig 4. UV-VIS spectra of Au-NPs **(a)** and Ag(s)-NPs **(b)** with maximum wavelengths at 536 and 420 nm, respectively. Different lines represent different concentrations. The middle panels present the magnified areas of NPs peaks. The lower panels show linear regression analysis of the corresponding peaks of Au-NPs and Ag(s)-NPs at different concentrations.

Supplement Figure 5

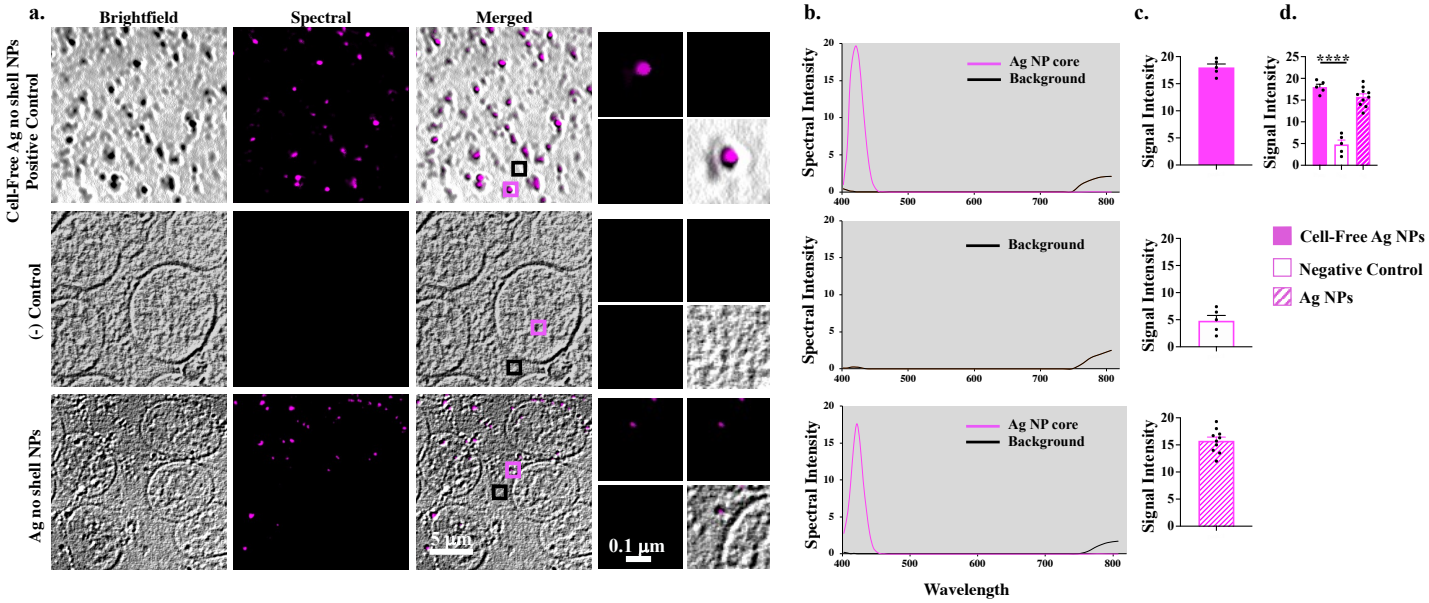

Supp Fig 5. Identification of Ag-NPs spectra

(a) Brightfield images are shown for Ag-NPs in the cell-free system (positive control), fixed cells (negative control), and 16-hour Ag-NPs-treated cells. The pseudo-colored spectral images were extracted from the spectra library for the Ag-NPs. Merged images exemplify superimposed brightfield and spectral images. The pink spectral image exhibits the core area of the Ag-NPs. **(b)** The graphs demonstrate the wavelength peaks of Ag-NPs clusters at ~420 nm for the positive control and the incubated cells. The pink wavelength presents the intensity of the core area. The black color displays the spectrum of the background area. The negative control spectra were identified based on unmatched spectra from our libraries. **(c)** The bar graphs show the variation of intensity data points at 420 nm. **(d)** The signal intensities were compared among cell-free positive control, non-treated cells negative control, and Ag-NPs-treated cells. N=4-5 for each positive and negative controls; N=8 for experimental groups. ****, P<0.0001.

Supplement Figure 6

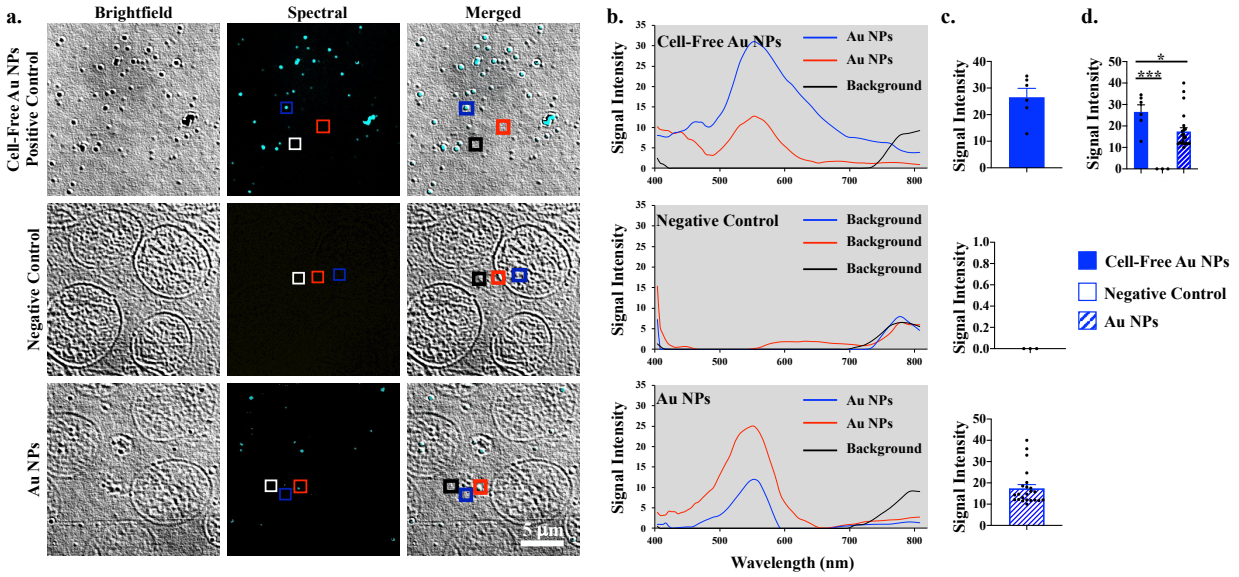

Supp Fig 6. Identification of Au-NPs spectra

(a) Brightfield images are shown for Au-NPs in the cell-free system (positive control), fixed cells (negative control), and 16-hour Au-NPs-treated cells. The pseudo-colored spectral images were extracted from the spectra libraries for Au-NPs. Merged images show combined brightfield and spectral images. **(b)** The graphs show the wavelength characteristics of the Au-NPs cluster at ~552 nm for the positive control and with cell incubation. Au-NPs graphs were shown after an automatic background subtraction by the software (**See Method**). The blue line displayed the area that contains higher wavelength intensity, and the red showed the region with less intensity. The background exhibited as a black color wavelength. The negative control graph shows the wavelengths. The negative control spectra were identified based on unmatched spectra from our libraries. **(c)** The bar graphs present the variation of intensity data points of the Au-NPs cluster peak of 552 nm. **(d)** The signal intensities were compared among cell-free positive control, non-treated cells negative control, and Au-NPs-treated cells. N=6 for each positive and negative controls; N=24 for experimental groups. *, P<0.05; ***, P<0.001.

Supplement Figure 7

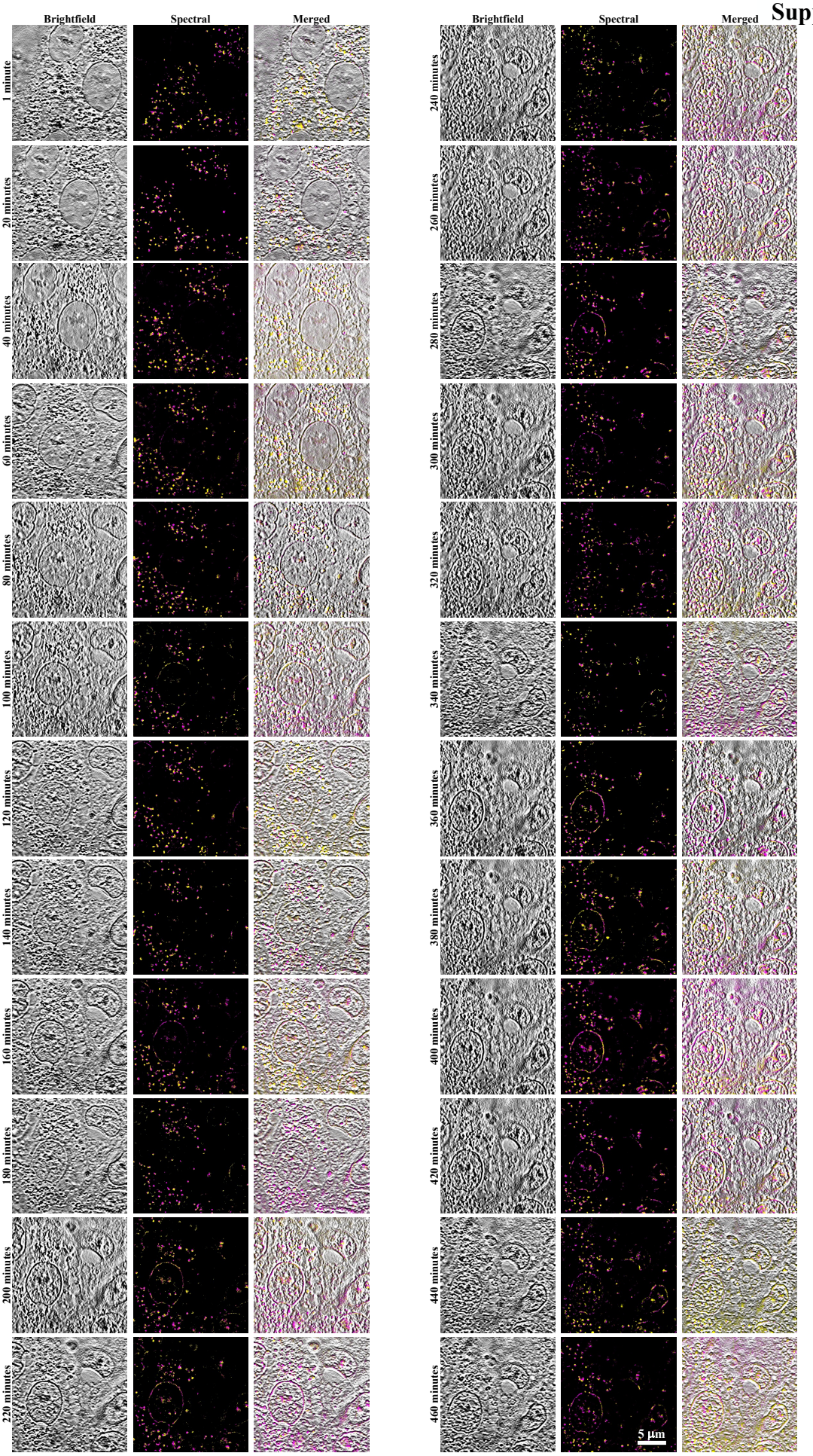

Supp Fig 7. Time-lapse imaging for the cells treated with 0.1 mg of Ag(s)-NPs in 2mL media. Images were captured every 20 minutes for about 8 hours. Over time, the number of Ag(s)-NPs increases in the nucleoplasm area.

Supplement Figure 8

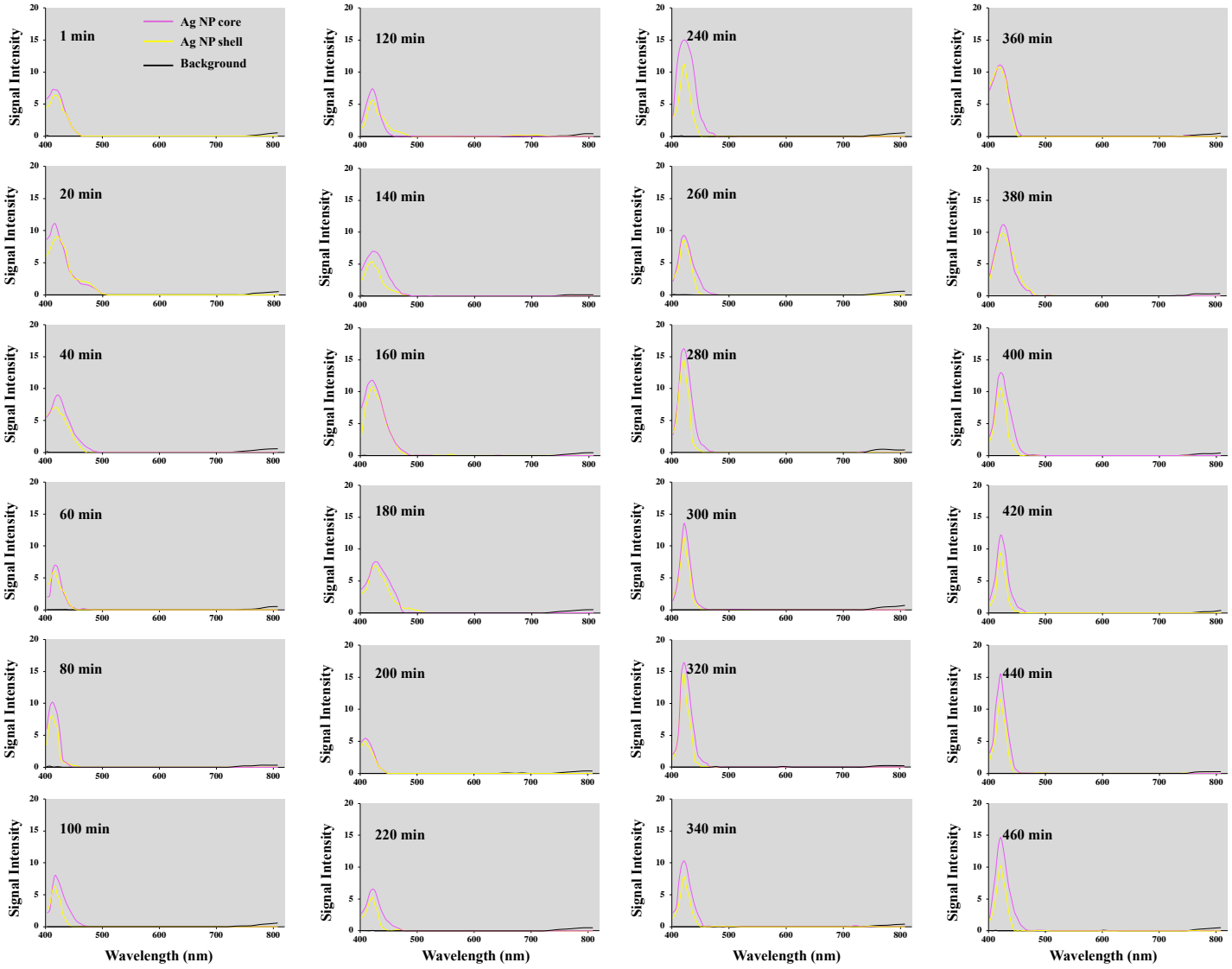

Supp Fig 8. Different graphs represent different Ag(s)-NP wavelengths. The pink lines represent the core area of Ag(s)-NPs, while the yellow lines show the shell of Ag(s)-NPs. The black lines represent the background area.

Supplement Figure 9

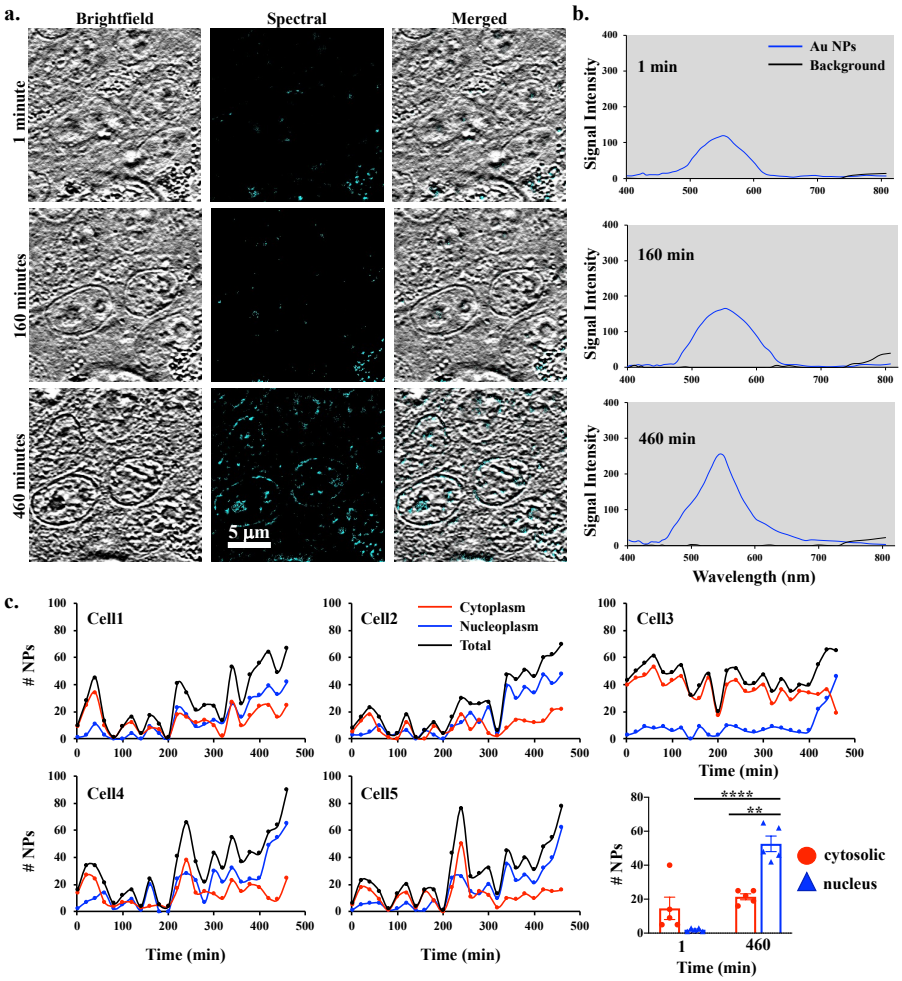

Supp Fig 9. (a) Sequential time imaging of cells treated with Au-NPs was captured for about 8 hours. Brightfield image and spectral scan were taken at every 20 minutes (**Supp Fig. 7**). **(b)** Spectral analysis was performed at the end of 8 hours after subtraction from the background spectra (**Supp Fig. 8**). **(c)** Line graphs illustrate the time-lapse analysis from 5 independent experiments. Number of Au-NPs (#NPs) was measured in one cell at each time point. Total #NPs were calculated from localization NPs in cytoplasm (outside nucleus) and nucleoplasm (inside nucleus) within a cell. Comparisons were done at the beginning (1 min) and end (460 min) of the 8-hour experiments. N=5. **, P<0.01; ****, P<0.0001.

Supplement Figure 10

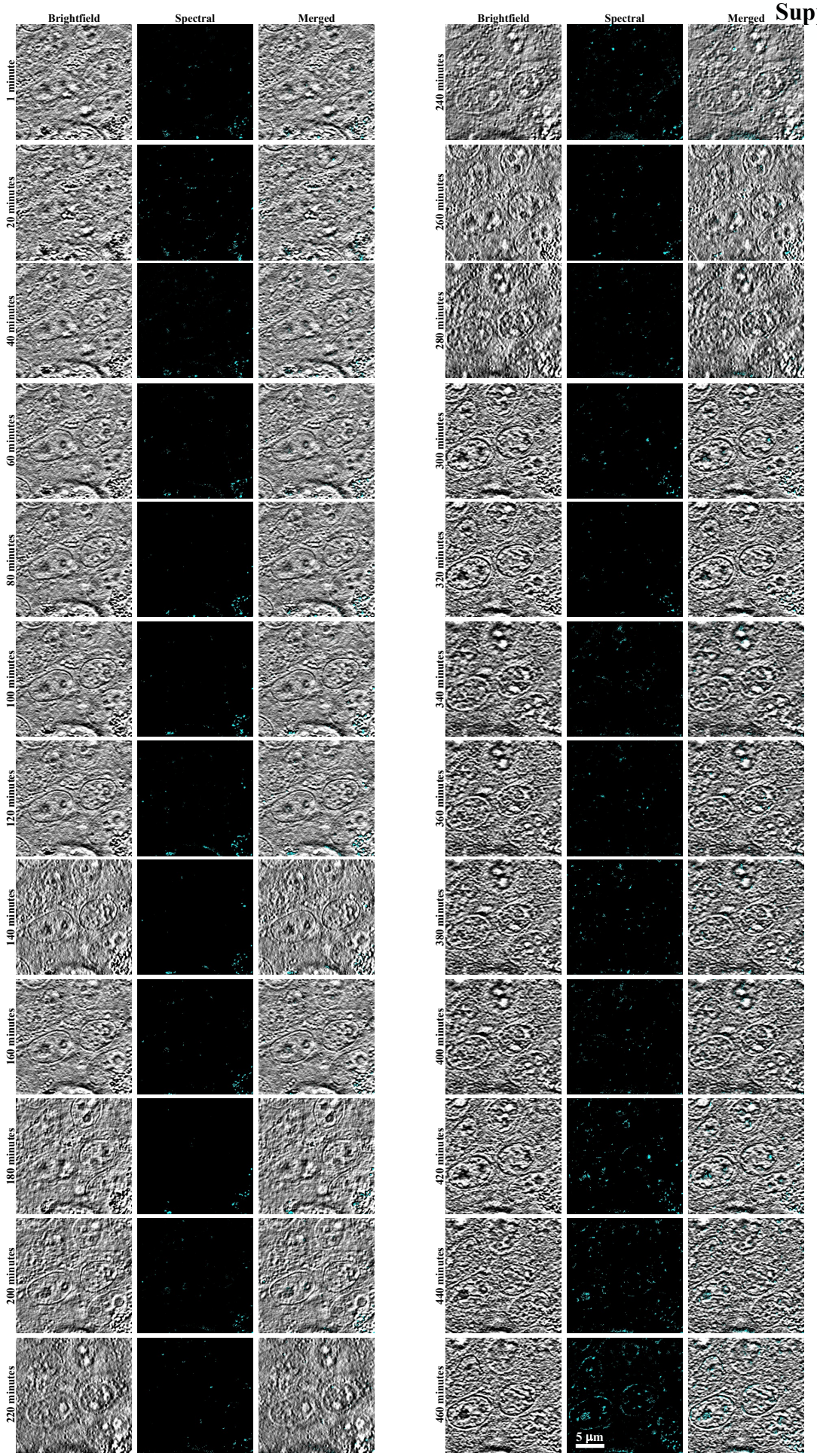

Supp Fig 10. Time-lapse imaging for the cells treated with Au-NPs. Images were captured every 20 minutes for 7 hours and 40 minutes. Over time, the number of Au-NPs increased in the nucleoplasm area.

Supplement Figure 11

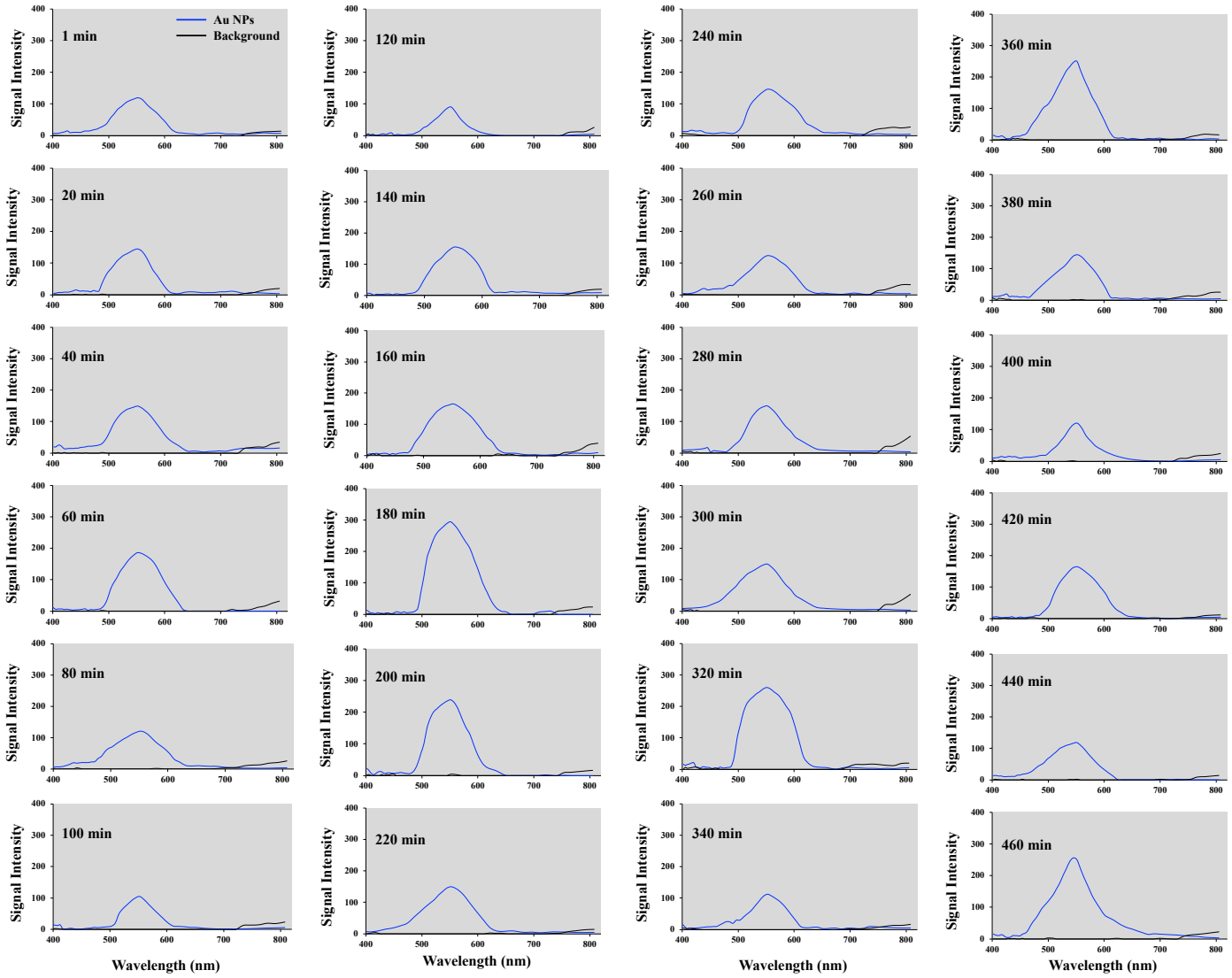

Supp Fig 11. Different graphs represent different Au-NPs cluster wavelengths with blue color, while black color exemplifies the background area.

Supplement Figure 12

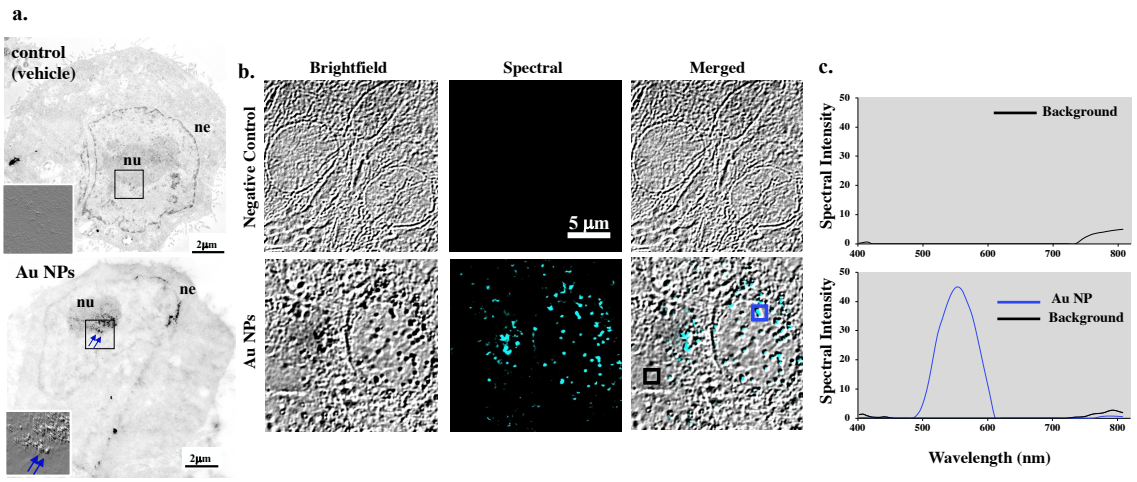

Supp Fig 12. (a) TEM analyses were performed after treatment of saline (control) or Au-NPs for 16 hours. An embossing filter was applied in some regions of cell nucleus for better clarity of the presence of NPs (insert with arrows). nu=nucleolus; ne=nuclear envelop. **(b)** Brightfield images of the silver stained non-treated (control) or 16 hours Au-NPs treated cells. The spectral images were extracted and pseudo-colored for the Au-NPs. Merged images revealed superimposed brightfield and spectral images to show the location of Au-NPs in the cell nucleus. **(c)** The spectral graphs clarify the wavelength peaks of Au-NPs at ~552 nm. N=5.

Supplement Figure 13

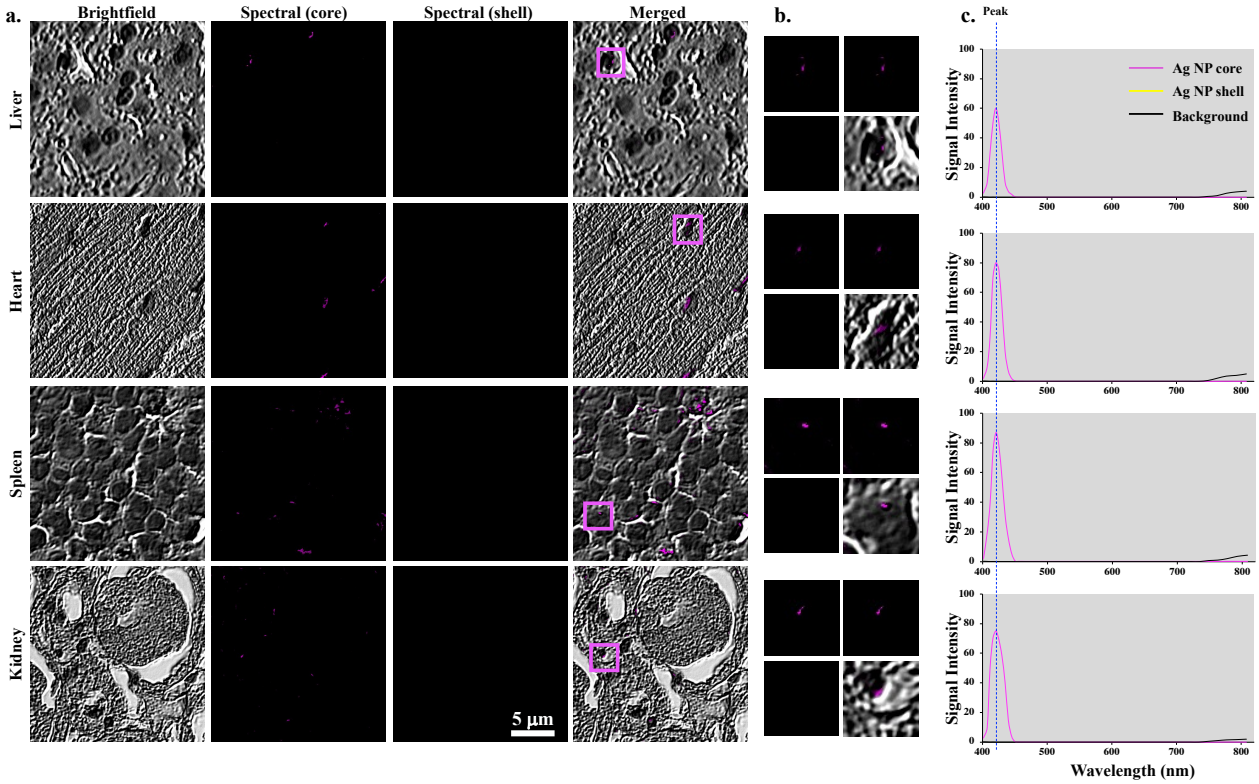

Supp Fig 13. (a) Brightfield images of the Ag-NPs in different organs tissues (liver, heart, spleen kidney) after intravenous injection of Ag-NPs for 24 hours. The spectral images were extracted from the spectra libraries for Ag-NPs. Merged images display combined brightfield and spectral images. **(b)** The Ag-NPs were shown in the pink pseudo-colored images. **(c)** The graphs reveal the wavelength characteristics of the Ag-NPs cluster at ~420 nm. The pink wavelength exhibits the intensity of the core area; the yellow wavelength displays the shell part. The background is shown as a black color wavelength. N=5.

Supplement Figure 14

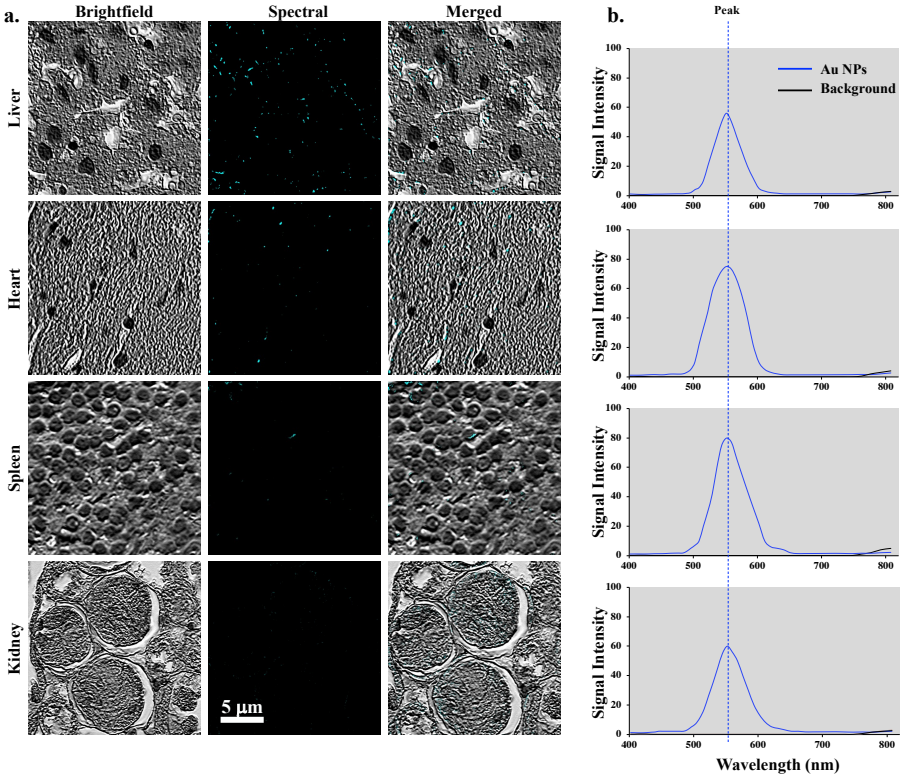

Supp Fig 14. (a) Brightfield images of the Au-NPs in different organs tissues (liver, heart, spleen kidney) after intravenous injection of Au-NPs for 24 hours. The spectral images were extracted from the spectra libraries for Au-NPs. Merged images display combined brightfield and spectral images. **(b)** The graphs reveal the wavelength characteristics of the Au-NPs at ~552 nm. The blue wavelength exhibits Au-NPs. The background is shown as a black color wavelength. N=5.

Supplement Figure 15

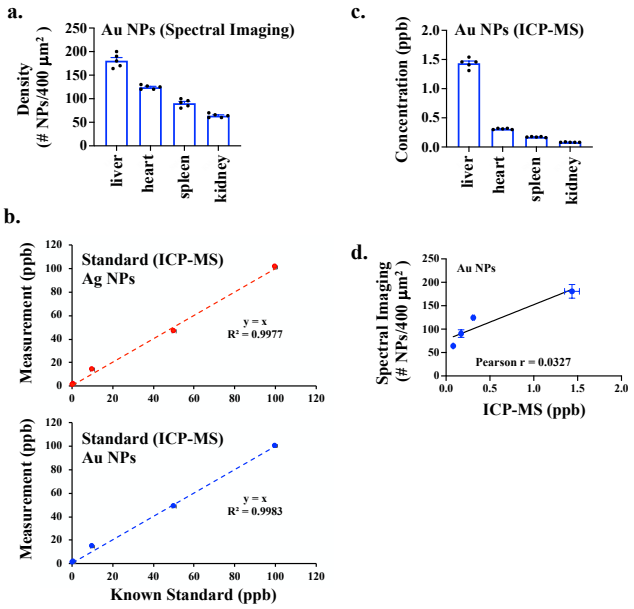

Supp Fig 15. (a) Tissue distribution of Au-NPs by spectral imaging is summarized in the bar graph. **(b)** Representative standard curves for ICP-MS are shown for Ag(s)-NPs and Au-NPs (0.5 to 100 ppb). **(c)** Tissue distribution of Au-NPs by ICP-MS is summarized in the bar graph. **(d)** The correlation analysis of the distribution of Au-NPs in different organs between ICP-MS and spectral imaging was performed. N=5 for each group.